Detecting targets with quantum microwave signals

David Vitali
School of Science and Technology,
Physics Division,
University of Camerino, Italy
Shabir Barzanjeh
Department of Physics and Astronomy
University of Calgary, Canada
Stefano Pirandola,
Department of Computer Science
University of York, UK
Johannes Fink
Institute of Science and Technology Austria
3400 Klosterneuburg, Austria

Sh. Barzanjeh et al., Sci. Adv. 6, eabb0451 (2020).

Outline

- **Quantum illumination:** protocol for target detection; an example of **quantum sensing** and its advantages

- It is a binary detection, rather than positioning, protocol; **target presence or absence**

- **quantum advantage over classical strategies** via **optimal quantum state discrimination**; determination of the optimal input state and optimal detection scheme

- **Experimental demonstration with a microwave entangled source** and digital postprocessing reproducing a phase-conjugate receiver, **Sh. Barzanjeh et al., Sci. Adv. 6, eabb0451 (2020). An important step toward a "quantum radar"**

Standard classical target detection

- single probe beam (e.g. coherent state) sent into a noisy region to detect the eventual presence of an object.
- (a) **Target present** $\Rightarrow$ small chance a reflected signal is detected; (b) **Target absent** $\Rightarrow$ the probe is lost and receiver sees only noise.

Typical scenario:

i) **Low reflectivity** $\Leftrightarrow$ high loss $\eta << 1$

ii) **Weak transmission** $\Leftrightarrow$ low signal $n_s << 1$

iii) **Bright background** large noise $n_b >> 1$

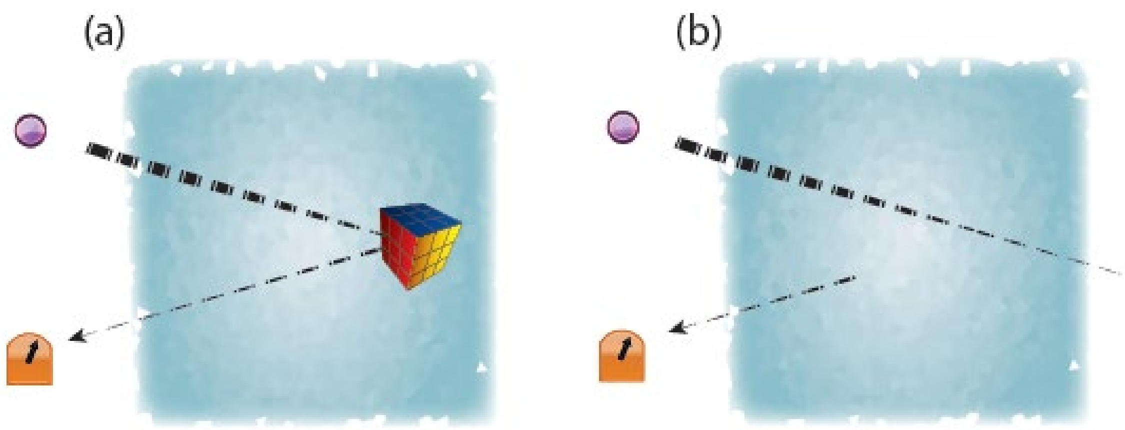

LOW SNR, i.e., **typical radar detection regime**

Classical binary detection problem

- Discrimination between two hypotheses ***H_0* (no target)** and ***H_1* (target present)**
- ***H_0*** $\Rightarrow$ return mode a_R = thermal state with n_b mean photons and $\langle a_R \rangle = 0$
- ***H_1*** $\Rightarrow$ return mode a_R = thermal state with n_b mean photons and $\langle a_R \rangle = \sqrt{\eta\, n_s}$

- **Optimal classical strategy**: i) optimal input state = **coherent state;** ii) optimal detection = **quadrature *X_i* measurement with homodyne**
- send *M>>1* modes and measure $X = \sum_{i=1}^{M} X_i$ $\Rightarrow$ distinguishing between two Gaussians shifted by $x_1 = M(\eta\, n_s)^{1/2}/2$

Classical binary detection problem II

- The standard strategy is to minimize the probability of error, $P_E=P_F+P_M$

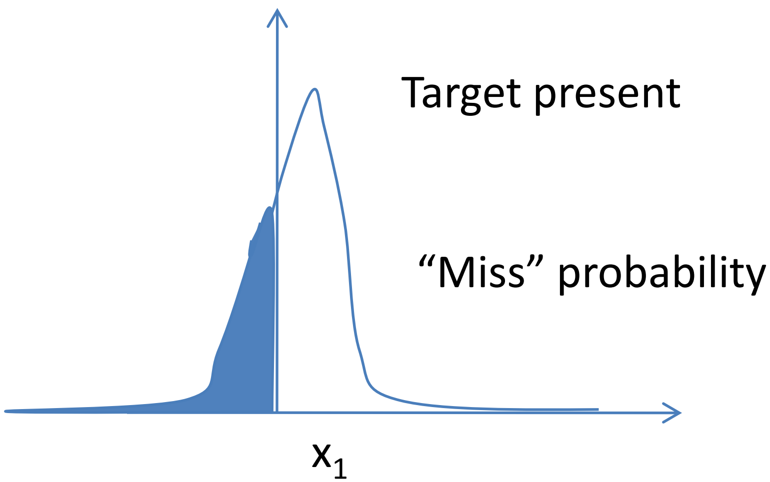

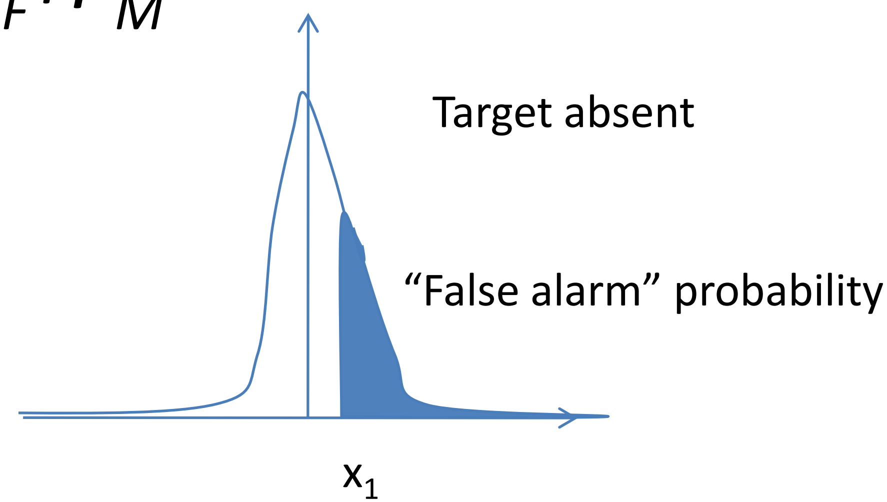

Minimum probability of error (MPE) =

$$P_e^{\min} = \frac{1}{2} erfc\left[\sqrt{\frac{\eta n_s M}{4 n_B + 2}}\right] = \frac{1}{2} erfc\left[\sqrt{\frac{SNR_c}{4}}\right]$$

$$SNR_c = \frac{\eta n_s M}{n_B + 1/2}$$

$$P_e^{\min} \approx \frac{\exp[-MR_c]}{2\sqrt{\pi M R_c}} \qquad for \quad M >> 1$$

$$R_c \approx \frac{\eta n_s}{4 n_b}$$

Classical error rate exponent

Quantum illumination protocol

- Different input state: two **maximally-entangled beams**, one is kept (idler) and the other one sent for target detection (signal).
- The reflected signal and idler are finally detected by an **appropriate joint measurement**.
- the use of an entangled source yields better performance, even though entanglement fails to survive the return trip.

S. Lloyd, Science, 321, 1043 (2008)
S.-H. Tan et al., Phys. Rev. Lett. 101, 253601 (2008).
S. Guha and B. I. Erkmen, Phys. Rev. A 80, 052310 (2009).
C. Weedbrook et al., New J. Phys. 18 043027 (2016)

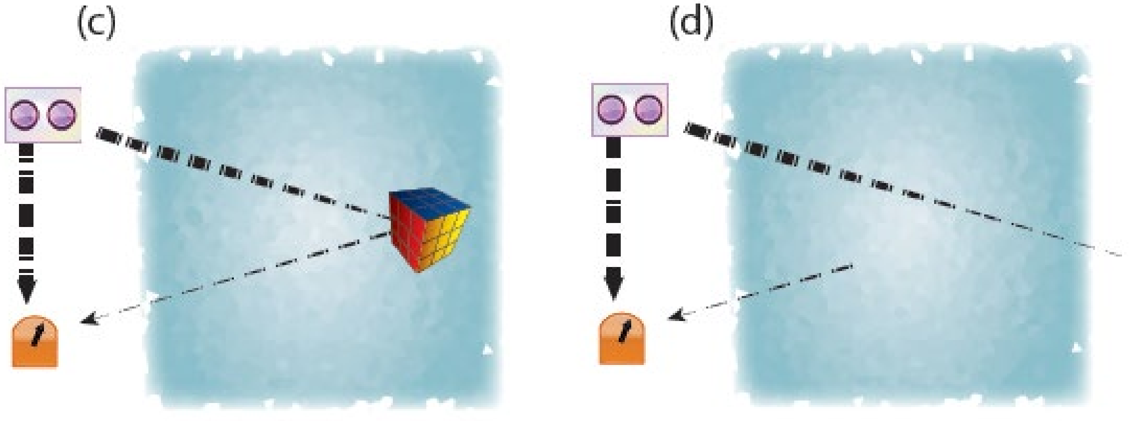

Quantum ideal case

- Optimal input state = **Two-mode squeezed state of a signal and idler** (G. De Palma & J. Borregaard, Phys. Rev. A 98, 012101 (2018))

$$\boxed{|\psi\rangle_{SI} = \sum_{n=1}^{\infty} \sqrt{\frac{\bar{n}_s^{\,n}}{(\bar{n}_s+1)^{n+1}}}\, |n\rangle_S |n\rangle_I}$$

- $H_0 \Rightarrow$ return mode $a_R = a_B$, in a thermal state with $n_b >>1$ mean photons
- $H_1 \Rightarrow$ return mode $\boxed{a_R = \sqrt{\eta}\, a_s + \sqrt{1-\eta}\, a_B}$
- **Optimal binary detection (Helstrom)** with multicopies (*M>>1*): *maximum "distance" between the quantum (mixed) states related to the two hypotheses* $\Rightarrow$

$$\boxed{P_e^{\min} = \frac{1}{2}\left[1 - \frac{1}{2} Tr\left| \left(\hat{\rho}_{RI}^{0}\right)^{\otimes M} - \left(\hat{\rho}_{RI}^{1}\right)^{\otimes M} \right|\right]}$$

ρ_{RI}^{j} j= 0,1 joint states of the return-idler mode system for the two hyp.

QI ⇒ 6 dB gain in error exponent

$$P_e^{\min} \le \frac{1}{2}\inf_{0\le s\le 1} Tr\left[\left(\hat{\rho}_{RI}^{0}\right)^{s}\left(\hat{\rho}_{RI}^{0}\right)^{1-s}\right]$$

Quantum Chernoff bound exponentially tight at large M

$$P_e^{\min} \approx \frac{\exp\left[-MR_Q\right]}{2\sqrt{\pi M R_Q}} \qquad for \quad M >> 1$$

$$R_Q \approx \frac{\eta n_s}{n_b} = 4R_C$$

6 dB gain

Optimal quantum error rate exponent

This is theory: How to realize such **optimal quantum receiver** ? Which experimentally feasible **detection scheme** achieves (or at least approaches) the optimal quantum error rate exponent R_Q ?

Optimal proof-of-principle detection scheme (Q. Zhuang, Z. Zhang, and J. H. Shapiro, PRL 118, 040801 (2017))

The FF-SFG (feedforward sum frequency generation) scheme achieving Helstrom's optimal binary detection

Iteratively repeat K times, the following receiver

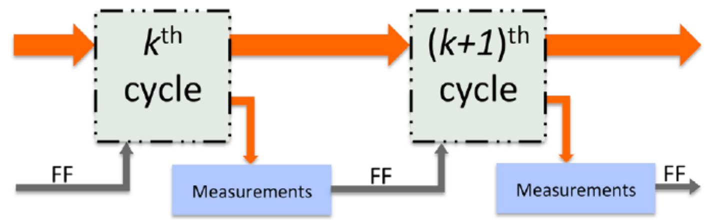

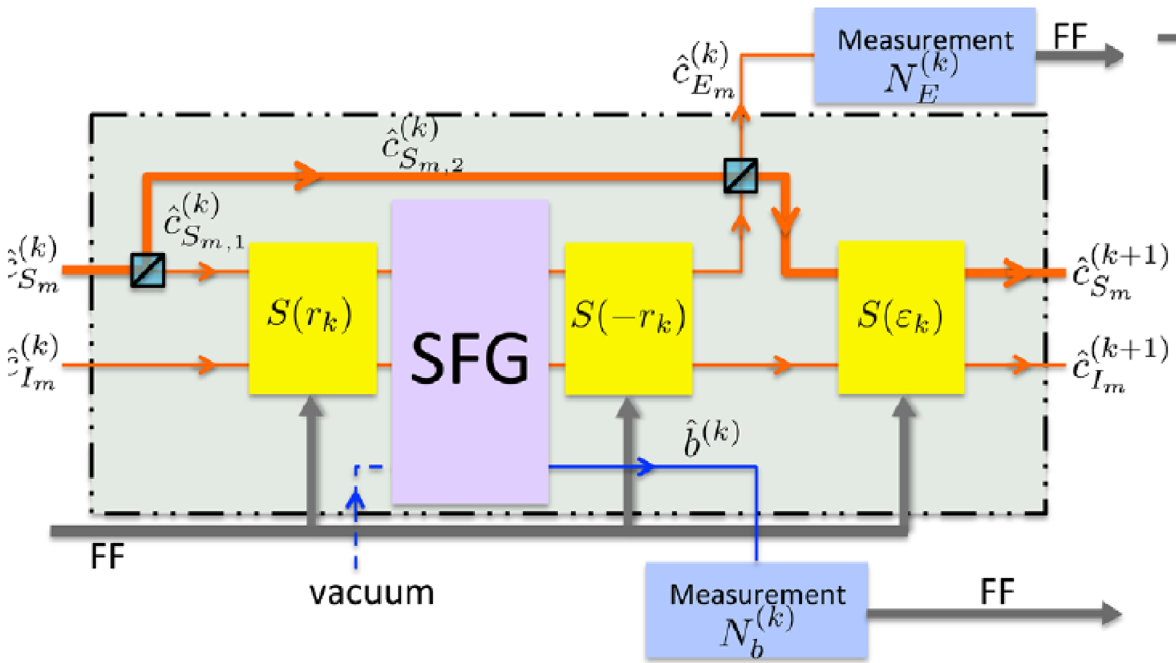

Measurement and feedforward

It is incredibly hard to implement

SFG

$$\hat{H}_I = \hbar g \sum_{m=1}^{M} (\hat{b}^\dagger \hat{a}_{S_m} \hat{a}_{I_m} + \hat{b} \hat{a}_{S_m}^\dagger \hat{a}_{I_m}^\dagger),$$

Sum-frequency generation: "time-inverted" parametric down conversion: M+1 modes coherent interaction, very hard to realize

Optimal mixed-state discrimination: it is known that it is achievable only with COLLECTIVE measurements and not with LOCC strategies

The SFG, **in the low-excitation limit of very small signal and idler photon number**, converts the signal-idler correlation into a nonzero amplitude of the sum-frequency (pump) beam *b(t)*

$$C(t) \equiv \langle \hat{a}_{S_m} \hat{a}_{I_m} \rangle_t$$

$$C(t) = C(0)\cos(\sqrt{M}gt),$$

$$b(t) = -i\sqrt{M}C(0)\sin(\sqrt{M}gt),$$

SFG maps the problem to the optimal discrimination of two coherent states (Dolinar receiver)

The three squeezers, the beam splitters, the measurements, and feedforward for K cycles are needed to reach this optimal low photon number regime

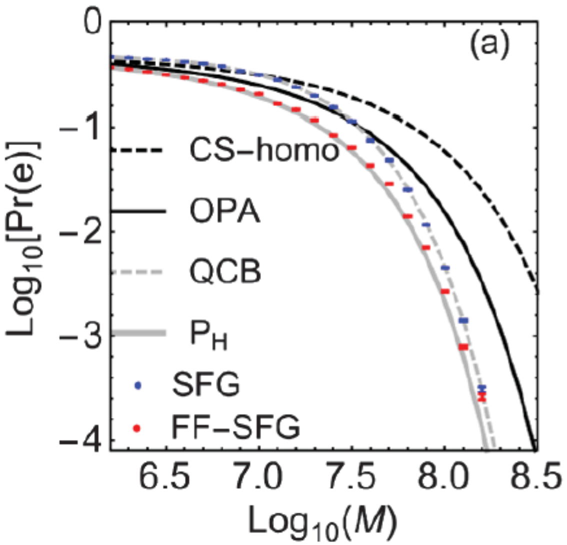

Phase conjugate receiver (PCR)

- **An easier to implement quantum receiver**

S. Guha and B. I. Erkmen, Phys. Rev. A 80, 052310 (2009).

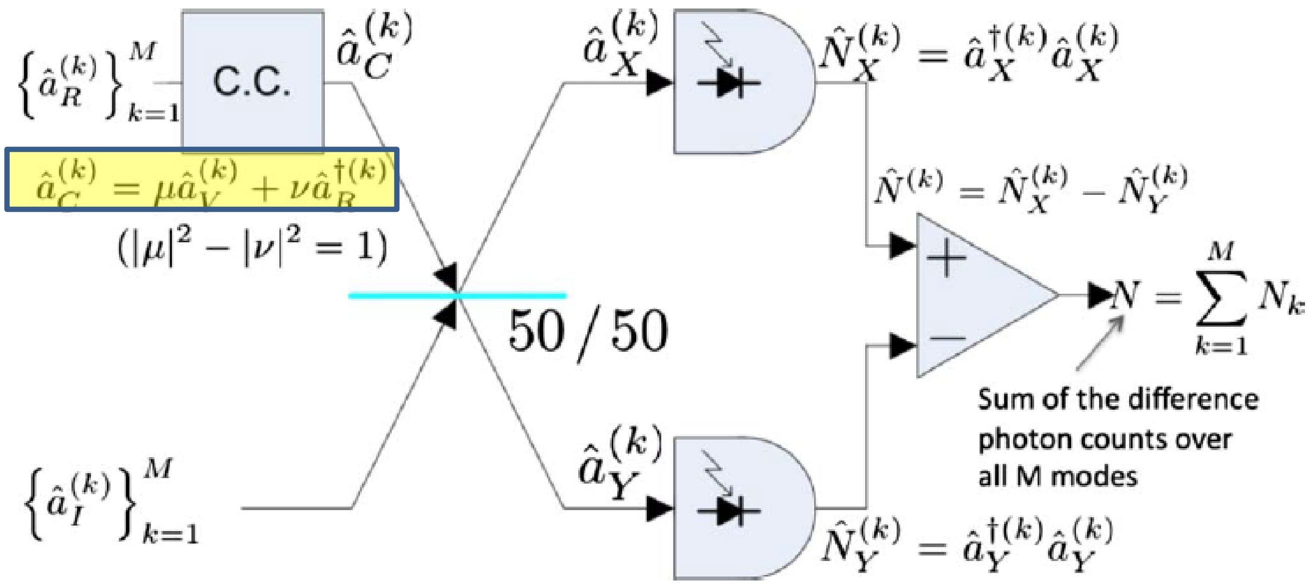

phase conjugation followed by balanced dual **photodetection**

$H_0 \Rightarrow \langle N_0 \rangle = 0;$

$H_1 \Rightarrow \langle N_1 \rangle = 2M \langle a_C^+ a_I \rangle \neq 0$

Phase-insensitive correlations, related to **signal-idler quantum correlations**

$$P_{\mathrm{QI}}^{(M)} = \frac{P_F + P_M}{2} = \frac{\operatorname{erfc}\left(\sqrt{\mathrm{SNR}_{\mathrm{QI}}^{(M)}/8}\right)}{2}$$

Error probability in the *M>>1* Central Limit Theorem Gaussian limit

$$P_e^{\min} \approx \frac{\exp\left[-MR_{PCR}\right]}{2\sqrt{\pi M R_{PCR}}} \quad for \quad M >> 1$$

$$R_{PCR} \approx \frac{\eta n_s}{2 n_b} = 2R_C$$

3 dB gain wrt classical case

In the usual scenario:

ι) $\eta << 1$

ii) low signal $n_s << 1$

iii) $n_b >> 1$

Not the optimal quantum 6 dB gain, but already significantly better than any classical target detection.

This is the detection strategy we have implemented experimentally by digital postprocessing

Experimental demonstrations

- QI has been first demonstrated at **optical wavelengths**, where **noise has been artificially added**

[E. D. Lopaeva et al., Phys. Rev. Lett. 110, 153603 (2013); Z. Zhang et al., Phys. Rev. Lett. 114, 110506 (2015)]

- **QI could be useful in radar applications at μ-waves, where one is easily in the low SNR regime**

- **First use of quantum entangled sources (with a Josephson parametric converter (JPC)) for target detection at μ-waves**

in C. W. Sandbo Chang et al., Appl. Phys. Lett. 114, 112601 (2019), and D. Luong et al., Trans. Aerosp. Electron. Syst. 10.1109/TAES.2019.2951213 (2019).

Heterodyne detection which is not optimal, and no quantum advantage clearly demonstrated

Our demonstration of microwave QI: employing a digital version of the phase-conjugated receiver

- We again use the **JPC entangled source of two-mode squeezed signal-idler** beams. Generated at **7 mK**

- By **postprocessing heterodyne data**, we digitally simulate the **phase-conjugate receiver (PCR)** giving a 3 dB rate-exponent gain, **Detection of a room-T target (up to 1 meter)**

- We **compare with the optimal classical detection (under the same conditions)**: coherent state & homodyne detection (passing through the same amplification/detection channel)

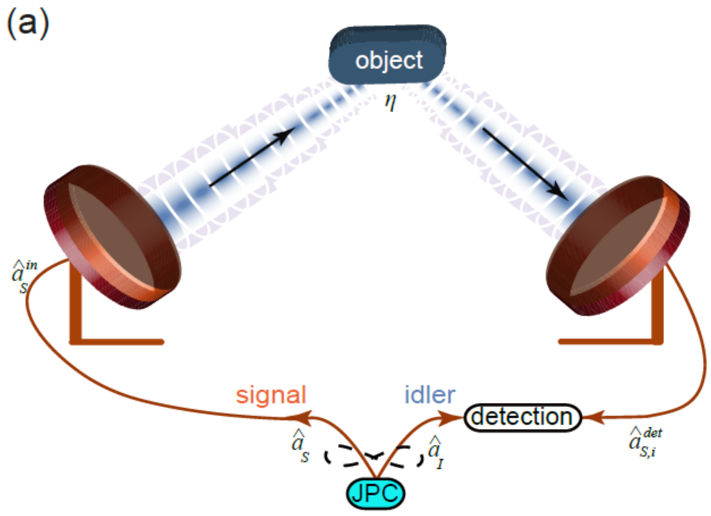

Schematics of the experiment

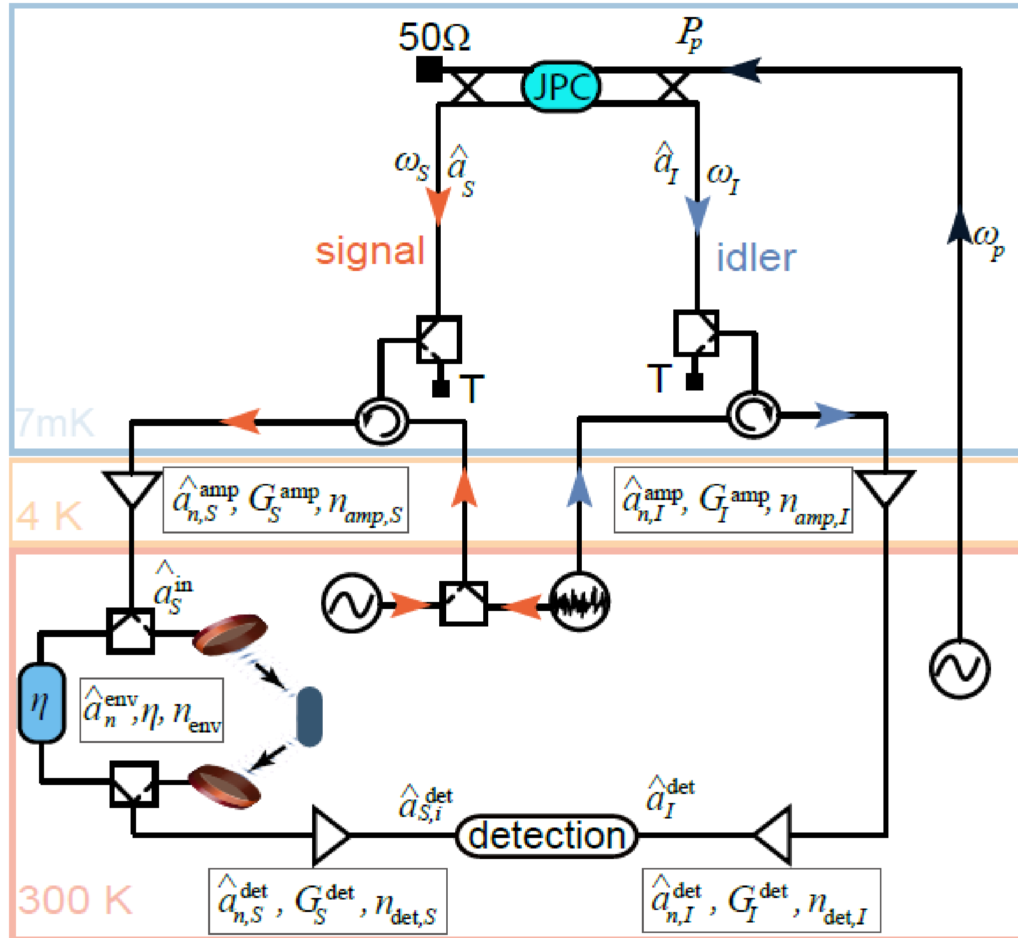

- The JPC output (or the reflected classical signals) **are amplified, down-converted, heterodyned, and digitized simultaneously and independently for both channels**.
- The signal mode passes through a room T measurement line with a switch used to select between a digitally controllable attenuator, and a free-space link realized with two antennas and a movable reflective object.
- Digital PCR: data postprocessing **with the ideal “calibrated” idler a_I**, obtained rescaling by the measured gain and subtracting the added amplifier noise

Experimental SNR

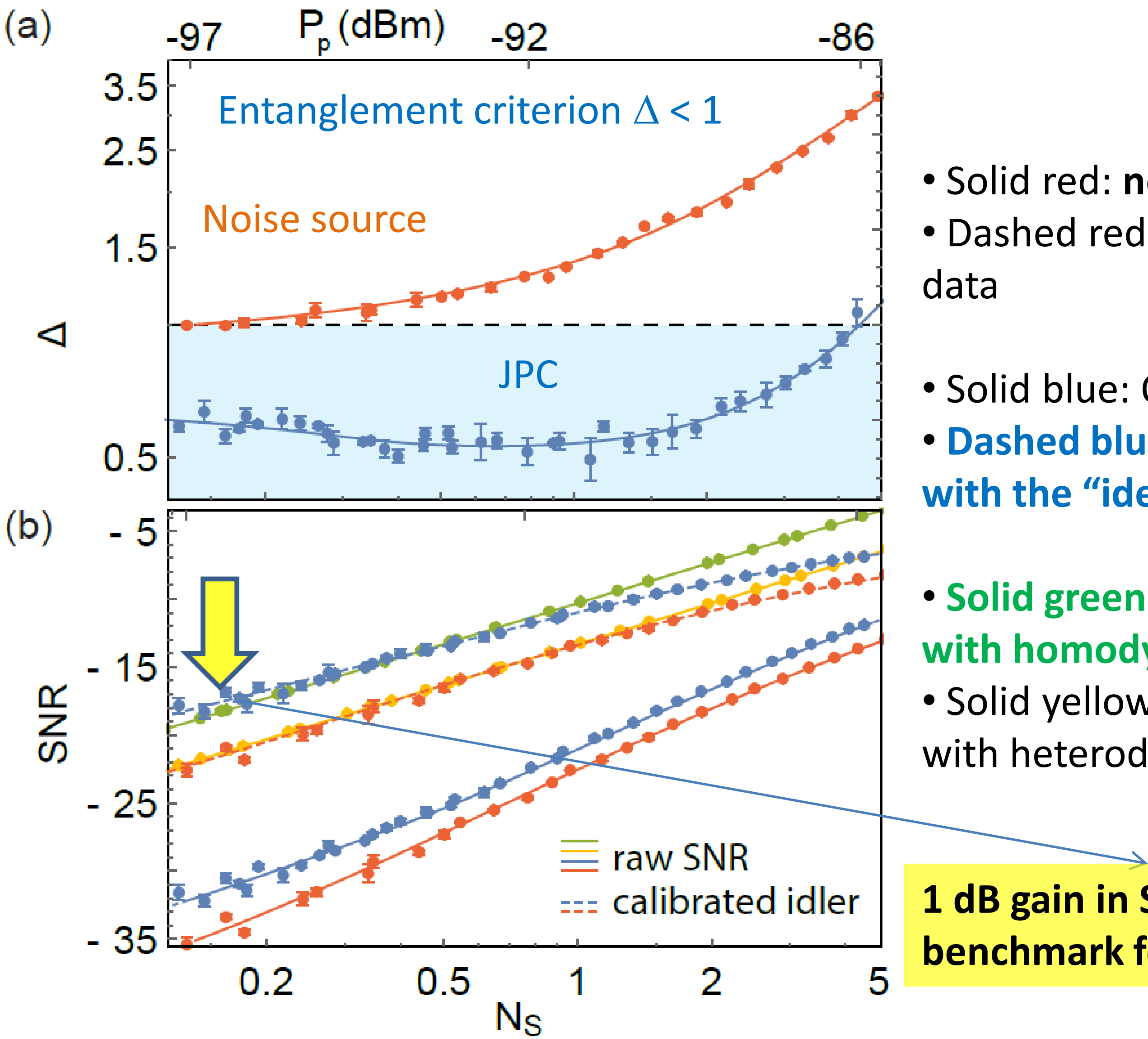

- Solid red: **noise radar**, amplified raw data
- Dashed red: noise radar, postprocessed data

- Solid blue: QI, amplified raw data
- **Dashed blue: QI, postprocessed PCR data with the "ideal" calibrated idler**

- **Solid green: coherent state illumination with homodyne (classical benchmark)**
- Solid yellow: : coherent state illumination with heterodyne

1 dB gain in SNR wrt to the classical benchmark for N_S < 0.4

Target detection

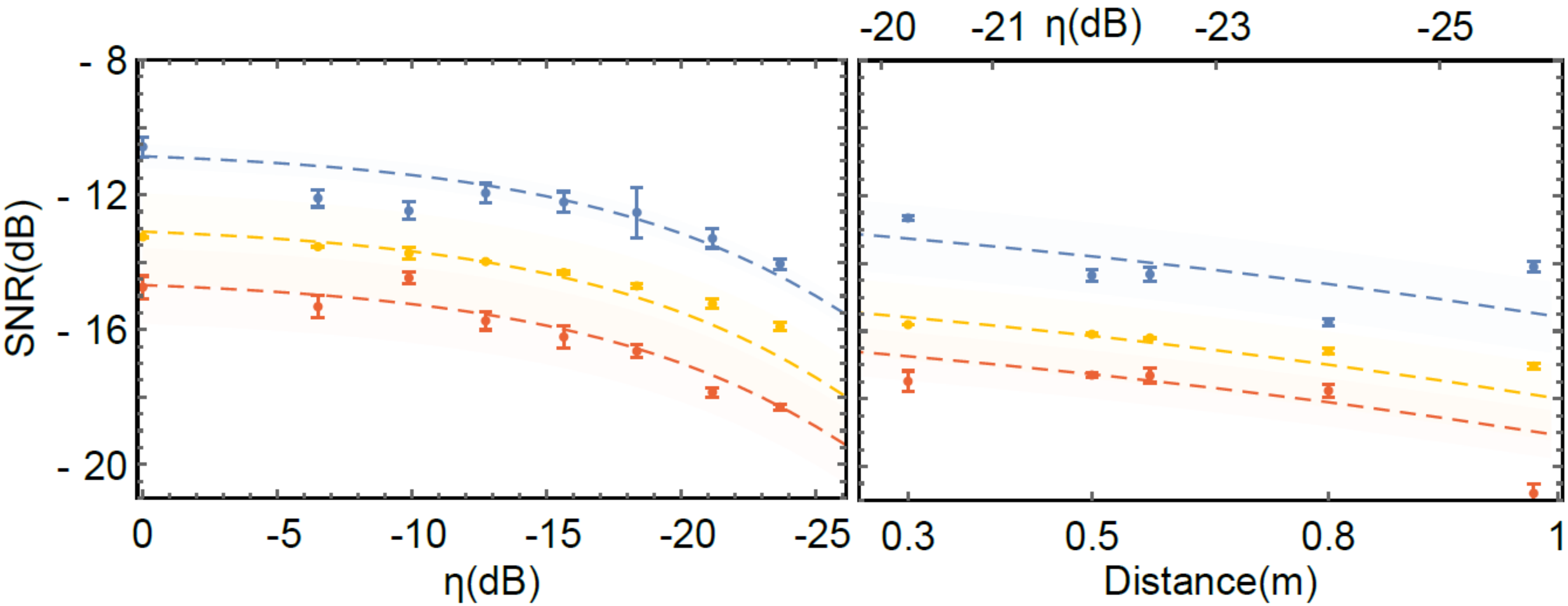

Experiment with a room T variable attenuator (η)

Experiment with a room T copper plate target and emitting and receiving antennas

1. **Blue**: QI = two-mode-squeezed state & digital PCR with calibrated idler
2. **Orange**: coherent state & heterodyne detection
3. **Red**: classical noise radar

Conclusions

- **Quantum illumination outperforms any classical target detection strategy**, expecially in low-signal/high-noise applications (e.g. radar systems). Up to 6 dB gain in error exponent-rate

- **We outperform the classical benchmark of coherent state and homodyne detection by 1 dB at low signal photon number, with entangled signal-idler beams and a digital post-processed phase-conjugated receiver, at short distance (< 1 meter)**

- Potential for **short-range radar applications** (security, automotive applications, medical imaging)

TECHNICAL SLIDES

Phase conjugate receiver with digital post-processing

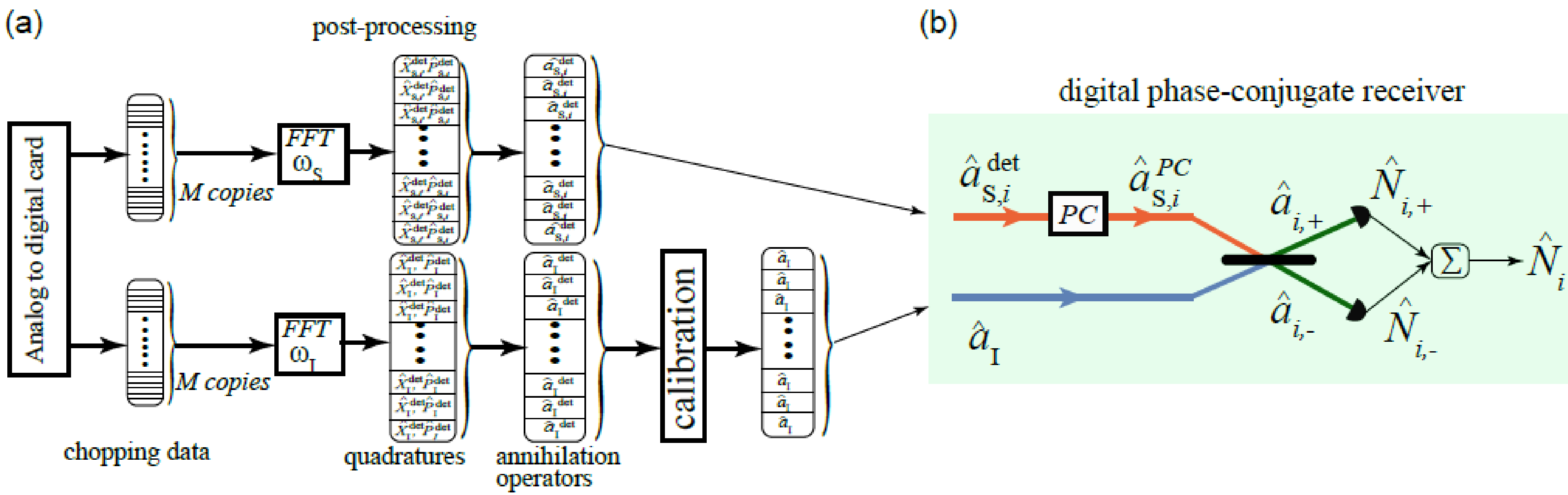

Digital PCR over the reconstructed signal and idler field operators

- **Optimal input probe quantum state: two-mode squeezed state** from a Josephson parametric converter (JPC).
- Comparison only with a **classical noise radar** (not the optimal classical strategy)
- **Detection is far from optimal**: linear heterodyne measurements and no joint idler-signal measurements

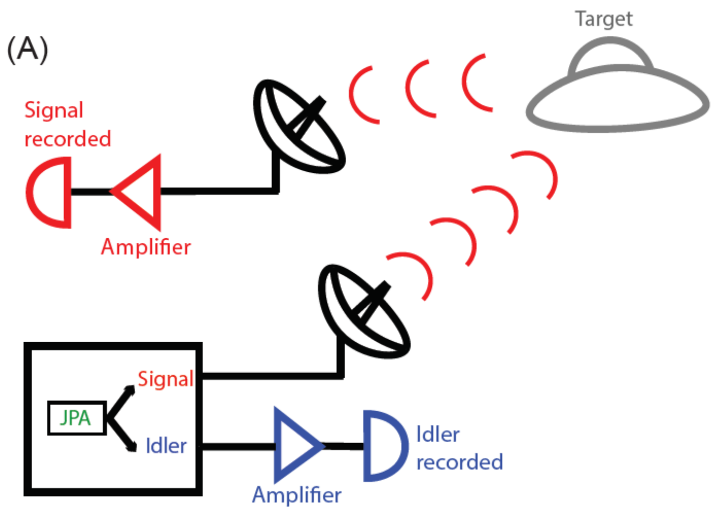

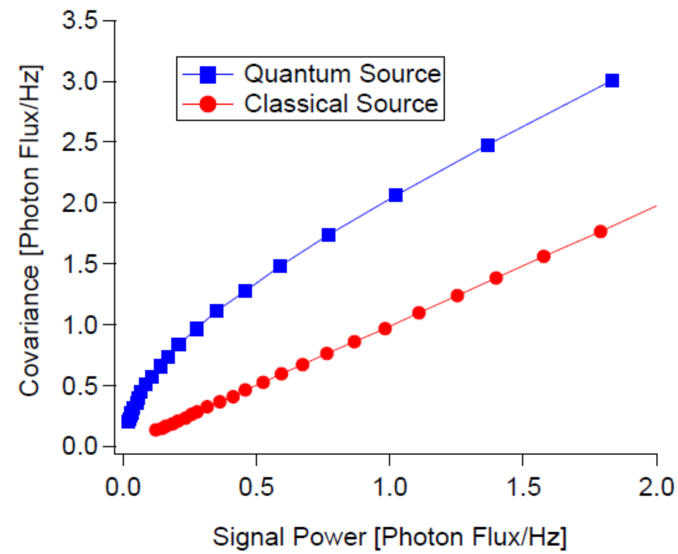

JPC: S-I correlations

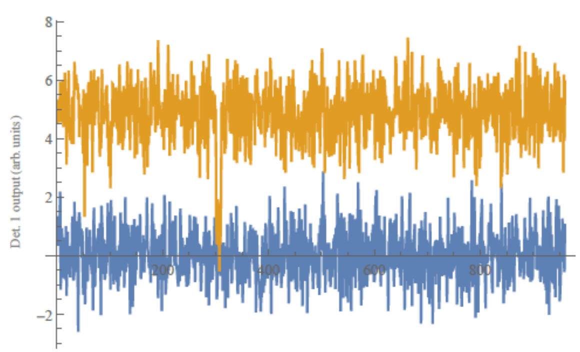

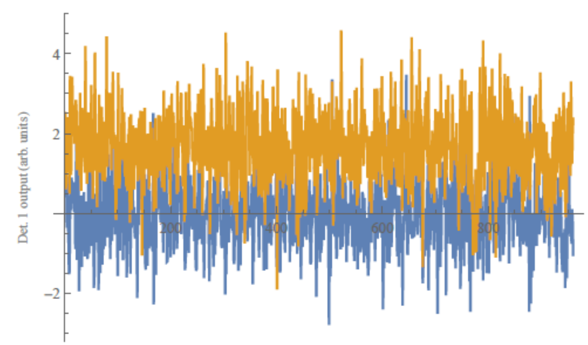

Gaussian noise: S-I correlations

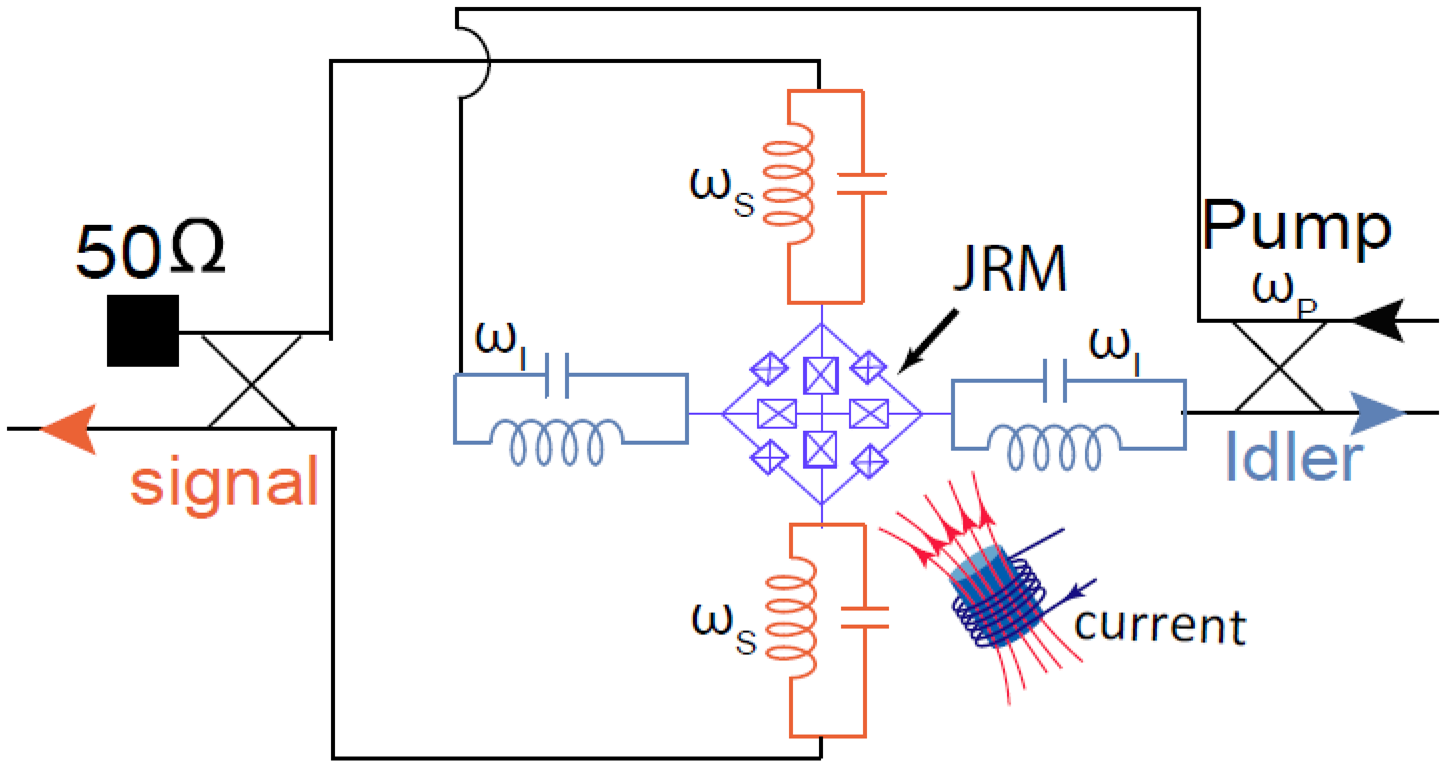

JPC = 4 + 4 Josephson Ring modulators + 3 resonant cavities. Gain 90 dB. 10 and 6.6 GHz

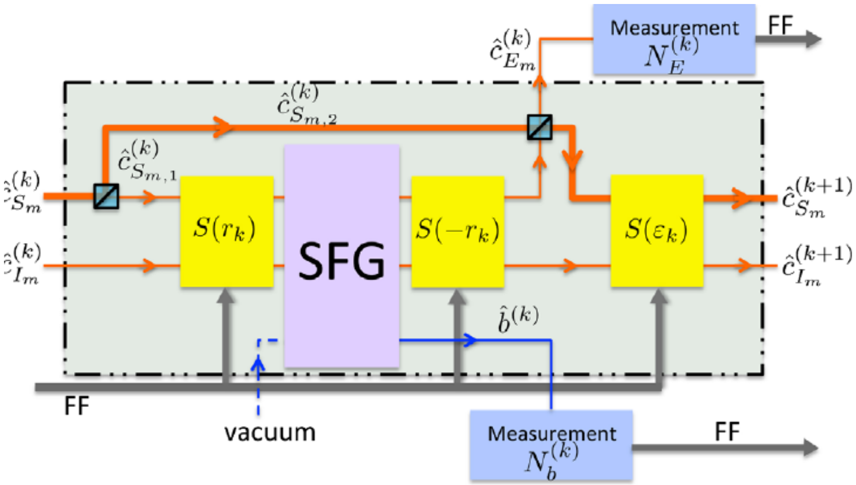

In each run, the squeezing parameters, r_k, ε_k are adjusted according to the results of the k-1 measurements and assuming one of the two options, H_0 or H_1,

1. The first beam splitter (with very low transmission) makes also the signal with low photon number as needed, (the idler is already low)
2. $S(r_k)$ cancels any eventual entanglement between s_m^k and I_m^k
3. If the assumed hypothesis is wrong, $b_k \neq 0$, is measured and it is corrected at the next cycle
4. Is determined by exploiting the fact that binary decision is equivalent to optimum discrimination between two coherent states (in this case for sum-frequency mode b, even though in a weak thermal environment)
5. The second squeezer guarantees that Nb and NE are roughly identical (Nb+NE is the quantity used to check if hypothesis is correct or not)
6. The third squeezer has $\varepsilon_k = \sqrt{t}\, r_k$, where t <<1 input BS transmission, in order to have at the end of each cycle

$$
\begin{aligned}
n_s^{\text{out}} &\simeq n_s^{\text{in}} \\
n_i^{\text{out}} &\simeq n_i^{\text{in}} \\
C_{si}^{\text{out}} &\simeq C_{si}^{\text{in}}[1 - \eta(1 + n_s^{\text{in}})].
\end{aligned}
$$

A typical simulation run over many cycles

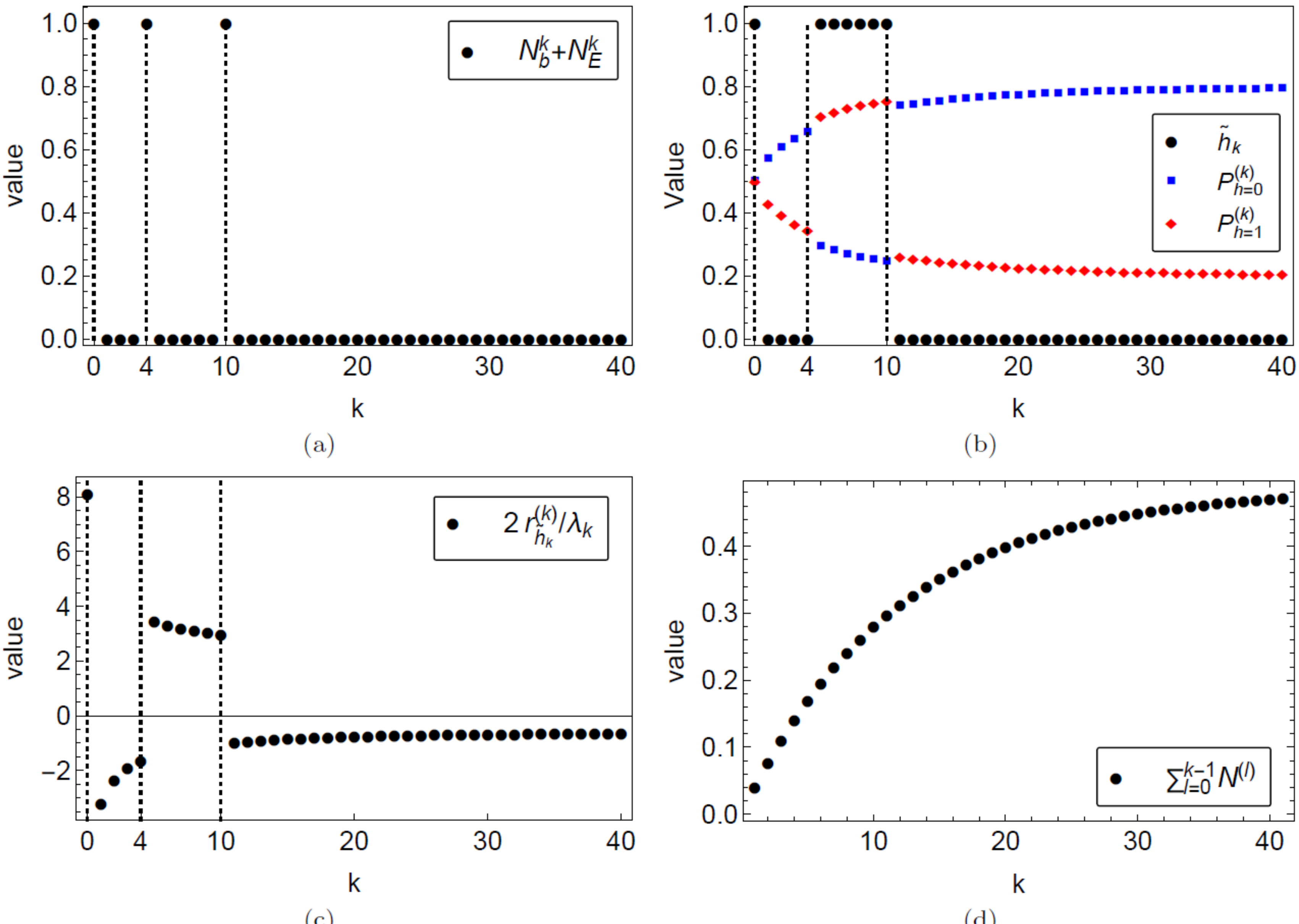

FURTHER REFINEMENT (Q. Zhuang, Z. Zhang, and J. H. Shapiro, arXiv:1703.02463v1)

1. The previous results exploit a **Bayesian approach** in which we assume that the two hypotheses (target present/absent) **have equal probabilities** at the beginning, and then updating the probabilities according to the result of the measurement and Bayes rule. In this context we have minimized the total error probability.

2. However, Bayesian analysis is not the preferred approach for target detection, owing to the **difficulty of accurately assigning prior probabilities to target absence and presence** and appropriate costs to false-alarm (Type-I) and miss (Type-II) errors. **Instead, radar theory opts for the Neyman-Pearson performance criterion, in which optimum target detection maximizes the detection probability, P_D = Pr(decide present|present), subject to a constraint on the false-alarm probability, P_F = Pr(decide present|absent).** (The detection probability satisfies $P_D = 1 - P_M$, where P_M =(decide absent|present) is the miss probability.)

This is achieved by adapting the previous scheme in the following way:

1. We fix a desired (low) value of the false alarm probability P_F.

2. We then apply the generalized Helstrom optimal binary decision for unequal prior probabilities π_0 and π_1, which minimizes the error probability (which now means minimizing P_M only), i.e.,

$$\boxed{P_e^{\min} = \frac{1}{2}\left[1 - \frac{1}{2} Tr\left|\left(\hat{\rho}_{RI}^{1}\right)^{\otimes M} - \frac{\pi_0}{\pi_1}\left(\hat{\rho}_{RI}^{0}\right)^{\otimes M}\right|\right]}$$

3. However, we do not know π_0 and π_1 and therefore we start from a ratio π_0/π_1 chosen at will and then we run the protocol in the same way, but with the differently initialized probabilities. It will converge in any case at the end.

4. The figure of merit in this Neyman-Pearson scenario is the ROC (receiver operating characteristic), i.e., P_D versus the initially chosen value of P_F.

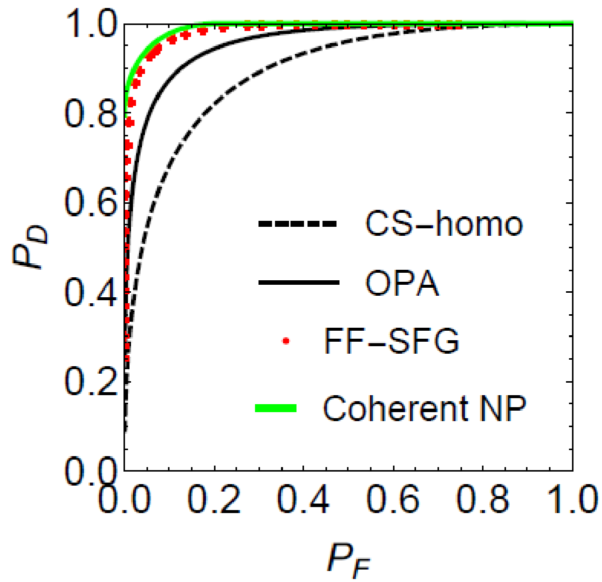

Figure 5. ROCs of QI target detection with FF-SFG reception (red dots), QI target detection with OPA reception (black solid curve), CI target detection with coherent-state (CS) light and homodyne reception (black dashed curve) schemes. Also included is the ROC of coherent-state Neyman-Pearson (Coherent NP) for discriminating between the coherent state $|\sqrt{M\kappa N_S/N_B}\,\rangle$ and the vacuum state (green solid curve), which is known to be realized by QI target detection with FF-SFG reception when $N_S \ll 1$. All four ROCs assume that $M = 10^{7.5}$, $N_S = 10^{-4}$, $\kappa = 0.01$, and $N_B = 20$.